Experimental L_{III}-shell hole widths in Yb and Ta

1990 J. Phys.: Condens. Matter 2 5619

(http://iopscience.iop.org/0953-8984/2/25/014)

J. Phys.: Condens. Matter 2 (1990) 5619–5626. Printed in the UK

Experimental L_{III}-shell hole widths in Yb and Ta

K Hämäläinen†, S Manninen†, S P Collins‡ and M J Cooper‡

† Department of Physics, University of Helsinki, Siltavuorenpenger 20D, SF-00170 Helsinki, Finland

‡ Department of Physics, University of Warwick, Coventry CV4 7AL, UK

Received 19 January 1990

Abstract. The resonant Raman scattering cross section from Yb and Ta was measured at incident photon energies close to the L_{III} absorption edge using synchrotron radiation. Assuming a constant density of final electron states the cross section has a simple dependence on the inner-shell hole width Γ, which yielded values of 5.3 eV and 5.7 eV for Yb and Ta L_{III}-shell hole widths, respectively. The error analysis gives an estimated accuracy of ± 0.2 eV. The present values together with a previous Ho result are slightly but systematically larger than the theoretical ones for the L_{III}-shell hole widths.

1. Introduction and theory

The energy width of an atomic inner shell depends on the total decay rate of transitions involving the inner-shell hole. In order to determine the energy width Γ the widths of the competing processes must be summed, i.e. the total width $\Gamma = \Gamma_R + \Gamma_A + \Gamma_{CK}$ where Γ_R is the radiative width, Γ_A the Auger width and Γ_{CK} the Coster–Kronig width. Most measurements of lifetime widths do not yield Γ directly, but it is obtained as a result of various experiments. The more frequently adopted alternative is to make a high resolution measurement of the x-ray emission line width which, after the separation of the instrumental broadening and the final state hole width, gives the core-level energy width. Despite tedious efforts the difference between the experimental data and the existing theories is often surprisingly large, especially in the case of L subshells as reviewed by Krause [1], Krause and Oliver [2] and McGuire [3].

In the previous work [4] we described an experimental method to determine the hole width Γ. It is based on measuring the scattered beam cross section while scanning the incident beam energy across the desired absorption edge. The elastic and inelastic scattering contribution (arising from the $\boldsymbol{A}^2$ term in the interaction Hamiltonian) can be minimised by using linearly polarised radiation and a scattering angle of 90°. The interaction is then governed by the $\boldsymbol{p}\cdot\boldsymbol{A}$ term and is referred to as resonant Raman scattering (RRS) below the absorption edge or fluorescence above it [4]. In the case of a KL transition (initial hole in the K shell) the cross section is

$$\left(\frac{d\sigma}{d\Omega}\right)_{KL} = \frac{(\Omega_K + \bar{\omega})}{4\pi^2\omega_1}\sigma_K(\Omega_K + \bar{\omega})\tan^{-1}\left(\frac{\Gamma_K/2}{\Delta E}\right) \tag{1}$$

providing the energy given to the ejected electron is large enough to allow neglect of the near edge effects. In equation (1) ω_1 is the incident photon energy, Ω_K the K-shell

0953-8984/90/255619+08$03.50

binding energy, $\bar{\omega}$ the average energy of the ejected electron, σ_K the K contribution to the photoelectric absorption, Γ_K the K-shell hole width and ΔE is the energy relative to the edge ($\Delta E = \Omega_K - \omega_1$). As shown previously [4] this equation can be used to determine the K-shell hole width Γ_K with an accuracy of about $\pm$ 0.1 eV with $\sim$ 1 eV incident beam resolution and using a solid state detector for the cross section measurement. The high resolution required in x-ray emission line width studies is not needed in this kind of experiment. In addition, the convolution with the higher shell hole widths has no effect on the total cross section.

Earlier results [4] indicated that the experimental K-shell widths (1.5 $\pm$ 0.1 eV for Cu and 1.9 $\pm$ 0.1 eV for Zn) agreed well with the theory [3,5]. On the other hand for the L_{III} subshell of Ho the experimental result of 4.8 $\pm$ 0.2 eV was slightly larger than the theoretical one of 4.3 eV [3,6]. It was therefore decided to examine the L-shell case more systematically to check whether this discrepancy is real or whether it could arise from an experimental error or from the model used in the analysis. In order to simplify the study the L_{III} edge was chosen because Coster–Kronig transitions are not allowed and fluorescence resulting from transitions to the other L subshells does not occur. L_{III} subshells having the absorption edges at low energies (less than $\sim$ 7 keV) were not accessible for experimental reasons and therefore Yb ($Z = 70$) and Ta ($Z = 73$) were chosen. Together with the previous result for Ho ($Z = 67$) this covers the range where the discrepancies between the rare experimental results are largest [3].

2. Experiment

The experimental work was done at the Daresbury synchrotron laboratory at the end station on beam line 7.6 which is 70 m away from the electron beam tangent point. The white synchrotron beam from the bending magnet was monochromated with a Si(111) channel-cut crystal and, due to the relatively low critical energy of 3.2 keV, the undesirable fluorescence excited by third and higher harmonics was undetectable. The pass-band of the monochromator was about 1.5 eV. The experimental set-up is shown schematically in figure 1. Previously [4,7] a separate measurement was needed to determine the absorption in the sample but in this case the absorption coefficient for the incident energy was measured at the same time using ion chambers before and after the sample foil. The scattered radiation was measured at a 90° scattering angle in the horizontal plane using a Si(Li) detector with an energy resolution of 180 eV at 8 keV. The energy spectrum of the scattered beam for each incident energy was recorded with a computer controlled multichannel analyser.

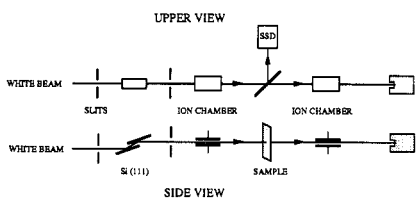

Figure 1. Experimental set-up (SSD = solid state detector).

The experimental L_{III}-shell hole width was determined for Yb and Ta where the corresponding electron binding energies are 8.944 keV and 9.881 keV, respectively.

The samples were 25×25 mm^2 polycrystalline foils as thin as commercially available (25 μm for Yb and 10 μm for Ta)—in order to make the attenuation measurement possible. A trial was made with 25 μm Er foil but it turned out to be too thick for the transmission measurement. The scattered radiation was measured with different incident energies ranging from 200 eV below up to 400 eV above the corresponding L_{III} edge. The measuring time varied from 30 s (above the edge) to 8 min (below the edge) per spectrum assuring statistical accuracy better than 1% in integrated intensities for each incident energy.

The measured spectra were corrected for the beam decay using the ion chamber current multiplied by $(\hbar\omega_1)^2$ to get the true photon flux hitting the sample [7]. The target foils were orientated symmetrically at an angle of 45° to the incident beam and the absorption correction was applied using the measured attenuation for the incident beam and values from the literature [8] for the scattered radiation. The experimental absorption edge jump ratios agreed with the literature values to within 1%. The use of the experimental values close to the edge where the absorption coefficient changes rapidly is essential since the precise position of the edge is unknown and the interpolation procedures might lead to a significant error. The attenuation measurement with two ion chambers gives the absorption coefficient corresponding exactly to the right incident energy. For the scattered radiation the absorption coefficient corresponding to the properly weighted mean value of $L\alpha_1$ and $L\alpha_2$ energies was used above the edge. Below the edge the value corresponding to the maximum scattered energy was used. The possible effects of this approximation are discussed in the next section. Before the integration small fluorescence peaks due to the rare-earth metal impurities were subtracted from spectra using a polynomial fit. Peaks from these trace impurities are strongly enhanced because their absorption edges are very close to the primary fluorescence lines excited above the desired L_{III} edge. The integrated intensity arising from the impurities was always less than 1% of the RRS intensities.

The measured differential cross section was integrated from 4 keV up to the maximum scattered RRS intensity. Thus the analysis included $L\alpha_1$, $L\alpha_2$ and $L\iota$ lines corresponding to the transitions $L_{III}M_V$, $L_{III}M_{IV}$ and $L_{III}M_I$, respectively. This is justified because according to the previous experiment [7] the branching ratios are the same above and below the absorption edge in the RRS region. In figure 2 a spectrum from the Ta sample shows the spectral lines used in the analysis and in figure 3 the measured cross section is plotted as a function of the incident energy. The measured count rates were not normalised to obtain the absolute scattering cross sections since in this analysis only the cross section relative to the full fluorescence level is needed.

3. Results and error analysis

The determination of the hole widths is based on energies close to the absorption edge where $\omega_1 \approx \Omega_K + \bar{\omega}$. The RRS cross section is isotropic to a good approximation and the energy relative to the L_{III} edge, ΔE, may be written as

$$\Delta E = \tfrac{1}{2}\Gamma_{L_{III}} \cot\left(\pi\sigma/\sigma_{L_{III}}\right) \tag{2}$$

where σ is the measured total RRS cross section and $\sigma_{L_{III}}$ the total fluorescence cross section, i.e. the full fluorescence level. A plot of the experimental data points based on this equation is shown in figure 4 and they lie accurately on a straight line. The

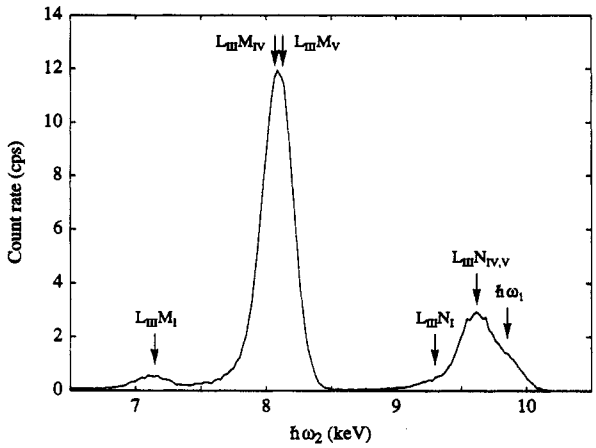

Figure 2. A typical RRS spectrum from Ta where the incident energy is 28 eV below the L_{III} absorption edge at 9.811 keV. The edge positions corresponding to different transitions involving the L_{III}-shell hole are indicated by arrows. Also, a small amount of elastic scattering can be seen around 9.8 keV.

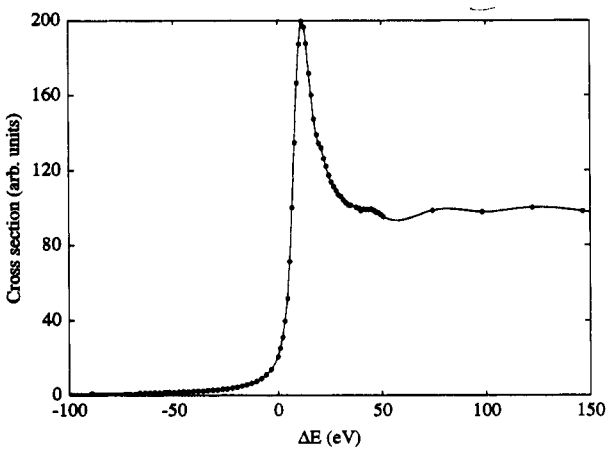

Figure 3. The measured scattering cross section for Ta relative to the L_{III} edge. Experimental data points are represented by circles and the full curve represents a spline fitting to the data points.

intersection of the line with the energy axis gives the edge position corresponding to the constant DOS model [4]. The slope of the line and thus Γ is determined by a linear fit using the energy range from 20 eV to 70 eV below the edge. The reasons for limiting the analysis to this region are discussed later. The hole widths derived are 5.3 eV for Yb and 5.7 eV for Ta. Comparison between the theory and experimental values is presented in table 1. The error $\pm$ 0.2 eV in the experimental values is based on the following estimations of error sources.

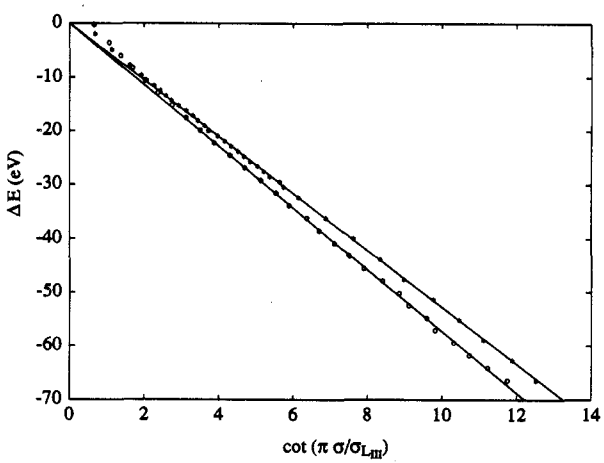

Figure 4. A plot of the experimental cross section according to equation (2). The upper line corresponds to Yb and the lower line to Ta. The slope of the curve gives the line width Γ. Deviation from the model can be seen close to the absorption edge.

Table 1. Comparison of experimental and theoretical L_{III}-shell hole widths.

	$\Gamma_{L_{III}}$ (eV)	Reference	
Ho	4.8 ± 0.2	[4]	Experimental
	4.3 ± 0.4	[2]	Semiempirical
Yb	5.3 ± 0.2	This work	Experimental
	4.7	[1,13]	Compiled from w_3 and Γ_R
	4.6 ± 0.5	[2]	Semiempirical
	5.1	[14]	Experimental
Ta	5.7 ± 0.2	This work	Experimental
	4.8	[1,13]	Compiled from w_3 and Γ_R
	4.9 ± 0.5	[2]	Semiempirical
	2.7	[14]	Experimental

3.1. Statistical accuracy

The statistical accuracy of the total cross section is always better than 1%. A small random deviation of the experimental data points from the straight line due to statistical fluctuations can be seen in figure 4 but it is negligible.

3.2. The density of states model

The effect of a constant DOS approximation was analysed with a model calculation using a step function DOS and a real one. As already pointed out in our previous paper [4] the constant DOS approximation only leads to differences closer than 10 eV to the edge. In the determination of Γ only points further than 20 eV from the edge were used and the constant DOS model should therefore not affect the experimental Γ value.

3.3. Monochromaticity

The incident beam has an energy resolution of 1.5 eV and long tails of the monochromator reflection curve could produce fluorescence below the edge and increase the

measured RRS cross section. However, after two reflections in a channel-cut monochromator the intensity drops as $(\Delta E)^{-4}$ where ΔE is the deviation from the Bragg peak energy. In this case the incident beam energy spread only affects the experimental Γ value if data points closer than a few eV below the edge are used.

3.4. The absorption correction

The absorption correction for the scattered beam was made using the coefficient corresponding to the maximum scattered beam energy. Close to the edge this is a good approximation since the RRS spectrum is sharply peaked, but further below the edge the RRS spectrum has a slowly decaying Lorentzian tail and an energy dependent absorption coefficient should be used. The justification for using a constant value is the poor energy resolution of the measuring system compared with the line width. According to a model calculation the difference between cross sections after the correct energy dependent absorption correction and approximation have been used is 1.5% at 20 eV, 5% at 70 eV and 20 % at 500 eV below the edge in case of 5 eV hole width. Thus, in the analysis, data points far below the edge were rejected.

3.5. The fluorescence cross section

The cross section for the full fluorescence above the edge is the most sensitive parameter in the analysis since RRS cross sections relative to this level, rather than the absolute values, are needed. The full fluorescence level was determined with a linear fit smoothing the EXAFS oscillations and other near edge structure. A change as small as 3% in the full fluorescence level leads to a $\pm$ 0.2 eV difference in Γ value. In the case of a thick sample the absorption correction is proportional to the absorption coefficient, and thus determination of the exact jump ratio at the edge is crucial. As mentioned previously the experimental value for the jump ratio agreed to better than 1% with the literature value and is therefore reliable. The approximated 3% uncertainty in the full fluorescence level is the main source of the ambiguity and gives the estimated $\pm$ 0.2 eV error limit to the line widths.

4. Discussion

The values of the L_{III} line widths given in table 1 can now be compared with the previous experimental and theoretical results. In the case of the rare-earth metals this can be done only by combining existing results for the fluorescence yield w_3, the radiative width Γ_R and the Auger width Γ_A to obtain $\Gamma = \Gamma_R/w_3$ or $\Gamma = \Gamma_R + \Gamma_A$. Experimental values for the L_{III} fluorescence yield have been mainly obtained using a coincidence technique in radioactive decay. For Yb there is good agreement between the measured values for w_3 (0.183 $\pm$ 0.011 [9], 0.20 $\pm$ 0.02 [10]) and the interpolated semiempirical result (0.210 [1]). In the case of Ta experimental values of 0.228 $\pm$ 0.013 [9], 0.235 $\pm$ 0.018 [11], 0.25 $\pm$ 0.03 [10] and 0.254 $\pm$ 0.025 [12] for w_3 have been reported, whereas the semiempirical plot gives 0.243. Combined with the relativistic Hartree–Fock calculations [13] for the L_{III}-subshell radiative width (0.947 eV for Yb, 1.163 eV for Ta), values of $\Gamma_{L_{III}}(Yb) = 4.7\,eV$ and $\Gamma_{L_{III}}(Ta) = 4.8\,eV$ are obtained when the semiempirical values of w_3 are used. Based on this kind of information the semiempirical level widths for K and L shells have been calculated [2] and including the estimated uncertainties the values of $\Gamma_{L_{III}}(Yb) = 4.6 \pm 0.5\,eV$ and $\Gamma_{L_{III}}(Ta) =$

4.9 ± 0.5 eV were obtained. Our results (including the earlier $\Gamma_{L_{III}}(\mathrm{Ho}) = 4.8 \pm 0.2$ eV compared with the semiempirical 4.3 ± 0.4 eV) show a small but systematic difference in each case. The compiled experimental widths given by Sevier [14] are 5.1 eV for Yb, very close to the present result, but only 2.7 eV and 3.5 eV for Ta. A summary of the experimental and theoretical hole widths including our previous Ho result is given in table 1.

Another interesting relationship is the spectral distribution of the scattered radiation compared with the density of unoccupied electron states above the Fermi level. This kind of technique has been widely used as an alternative to EXAFS. Close to the absorption edge the details are dominated by the density of unoccupied states which can be calculated from the band structure. According to the dipole approximation only the transitions to the s- or d-like states are allowed because we are now dealing with 2p electrons. In the case of Ni it was shown [7] that, using the calculated partial density of 2p states, the observed fine structure in the scattering cross section of the K-edge scan was well explained.

A few attempts to correlate the white line structure of rare-earth metals with the density of states have been made [15–19] but the results are conflicting if the position of the white line is considered. The existence of the white line in L_{II} and L_{III} absorption spectra but not in the L_I is a common feature, which in terms of the dipole approximation suggests that transitions to the unoccupied 5d states are responsible. The existing band structure calculations for Ta [20–22] all give similar kinds of densities of states showing a sharp peak at about 5 eV above the Fermi level and another smaller one centred at 15 eV. The partial densities of states given by Papaconstantopoulos [22] show that the 5 eV peak is really due to the d states, confirming the dipole approximation suggestion. A comparison with figure 3 shows that the energy difference between the first two peaks is about 10 eV as predicted by the theory. The first peak is located at about 10 eV above the absorption edge and the deviation from the theory is probably due to the difference in energy scale which has been fixed in this case by our constant DOS model to obtain Γ. The experimental half width of the white line, which is independent of the edge position, is approximately 8.7 eV. This agrees quite well with a previous result of 9.7 eV [17] measured using a conventional x-ray tube and a crystal analyser.

We can conclude that the present method, based on the measurement of the scattering cross section, gives a more consistent set of data for both K and L_{III} shells than experimental techniques developed previously to study the inner-shell level widths. It can also be extended to study the L_I and L_{II} subshells and it is even possible to separate the Coster–Kronig contribution.

Acknowledgments

This work has been supported by the Finnish Academy (KH and SM) and SERC (SPC and MJC). The help of P Suortti, G Clark, D Laundy, D Timms, J Graeffe and S Mamauda is gratefully acknowledged.

References

[1] Krause M O 1979 *J. Phys. Chem. Ref. Data* **8** 307

[2] Krause M O and Oliver J H 1979 *J. Phys. Chem. Ref. Data* **8** 329
[3] McGuire E J 1975 *Atomic Inner Shell Physics* ed B Crasemann (New York: Plenum) p293
[4] Hämäläinen K, Manninen S, Suortti P, Collins S P, Cooper M J and Laundy D 1989 *J. Phys.:Condens. Matter* **1** 5955
[5] McGuire E J 1971 *Phys. Rev.* A **3** 587
[6] Walters D L and Bhalla C P 1971 *Phys. Rev.* A **3** 519
[7] Manninen S, Suortti P, Cooper M J, Chomilier J and Loupias G 1986 *Phys. Rev.* B **34** 8351
[8] Saloman E B, Hubbell J H and Scofield J H 1988 *At. Data Nucl. Data Tables* **38** 1
[9] Mohan S, Freund H U, Fink R W and Venugopala Rao P 1970 *Phys. Rev.* C **1** 254
[10] Jopson R C, Khan J M, Swift C D and Williamson M A 1963 *Phys. Rev.* **131** 1165
[11] Campbell J L, McNelles L A, Geiger J S, Merritt L S and Graham R L 1977 *Can. J. Phys.* **55** 868
[12] Price R E, Mark H and Swift C D 1968 *Phys. Rev.* **176** 3
[13] Scofield J H 1969 *Phys. Rev.* **179** 9
[14] Sevier K D 1972 *Low Energy Electron Spectrometry* (New York: Wiley)
[15] Padalia B D, Gupta S N, Vijayavargiya V P and Tripathi B C 1974 *J. Phys. F: Met. Phys.* **4** 938
[16] Gupta S W and Padalia B D 1971 *J. Phys. F: Met. Phys.* **4** 335
[17] Padalia B D and Gupta S N 1972 *J. Phys. F: Met. Phys.* **2** 189
[18] Agarwal B K and Agarwal B R K 1978 *J. Phys. C: Solid State Phys.* **11** 4223
[19] Dubey V S and Shrivastava B D 1972 *Phys. Status Solidi* b **53** K51
[20] Mattheiss L F 1970 *Phys. Rev.* B **1** 373
[21] Petroff I and Viswanathan C R 1971 *Phys. Rev.* B **4** 799
[22] Papaconstantopoulos D A 1986 *Handbook of the Band Structure of Elemental Solids* (New York: Plenum)